

Nano-loaded human umbilical cord mesenchymal stem cells as targeted carriers of doxorubicin for breast cancer therapy

Shunxiu Cao, Jiamin Guo, Yujing He, Murad Alahdal, Shanshan Tang, Yuekui Zhao, Zhaocong Yang, Huashan Gao, Wenjun Hu, Hulin Jiang, Lianju Qin & Liang Jin

To cite this article: Shunxiu Cao, Jiamin Guo, Yujing He, Murad Alahdal, Shanshan Tang, Yuekui Zhao, Zhaocong Yang, Huashan Gao, Wenjun Hu, Hulin Jiang, Lianju Qin & Liang Jin (2018) Nano-loaded human umbilical cord mesenchymal stem cells as targeted carriers of doxorubicin for breast cancer therapy, *Artificial Cells, Nanomedicine, and Biotechnology*, 46:sup1, 642-652, DOI: [10.1080/21691401.2018.1434185](https://doi.org/10.1080/21691401.2018.1434185)

To link to this article: <https://doi.org/10.1080/21691401.2018.1434185>



Published online: 19 Feb 2018.



Submit your article to this journal [↗](#)



Article views: 1521



View related articles [↗](#)



View Crossmark data [↗](#)



Citing articles: 9 View citing articles [↗](#)



Nano-loaded human umbilical cord mesenchymal stem cells as targeted carriers of doxorubicin for breast cancer therapy

Shunxiu Cao^{a*}, Jiamin Guo^{a*}, Yujing He^b, Murad Alahdal^a, Shanshan Tang^a, Yuekui Zhao^a, Zhaocong Yang^a, Huashan Gao^a, Wenjun Hu^a, Hulin Jiang^{b*}, Lianju Qin^{c*} and Liang Jin^{a*}

^aSchool of Life Science and Technology, China Pharmaceutical University, Nanjing, China; ^bDepartment of Pharmaceutics, China Pharmaceutical University, Nanjing, China; ^cFirst Affiliated Hospital, Nanjing Medical University, Nanjing, China

ABSTRACT

The main challenge of anticancer drugs is poor tumor targeting. Now cellular carriers are widely investigated to deliver anticancer agents. As an ideal cellular candidate, human umbilical cord derived mesenchymal stem cells (hUC-MSCs) possess inherent tropism potential to tumor. Here, we constructed hUC-MSCs carrying transferrin-inspired-nanoparticles that contain doxorubicin(hUC-MSCs-Tf-inspired-NPs) to achieve enhanced anti-tumor efficacy and made an evaluation. Results represented that hUC-MSCs-Tf-inspired-NPs not only exhibit the controlled-release property of Tf-inspired-NPs, but also integrate tumor tropism and penetrative abilities of MSCs. The tumor volume of nude mice bearing breast cancer MCF-7 treated with hUC-MSCs-Tf-inspired-NPs, was remarkably reduced compared to those treated with free drug or Tf-inspired-NPs. Thus, Tf-inspired-NPs loaded hUC-MSCs have a potential to deliver anticancer drugs.

ARTICLE HISTORY

Received 18 September 2017
Revised 23 January 2018
Accepted 25 January 2018

KEYWORDS

Mesenchymal stem cells
nanoparticles; artificial cells;
targeted delivery;
doxorubicin; breast cancer

Introduction

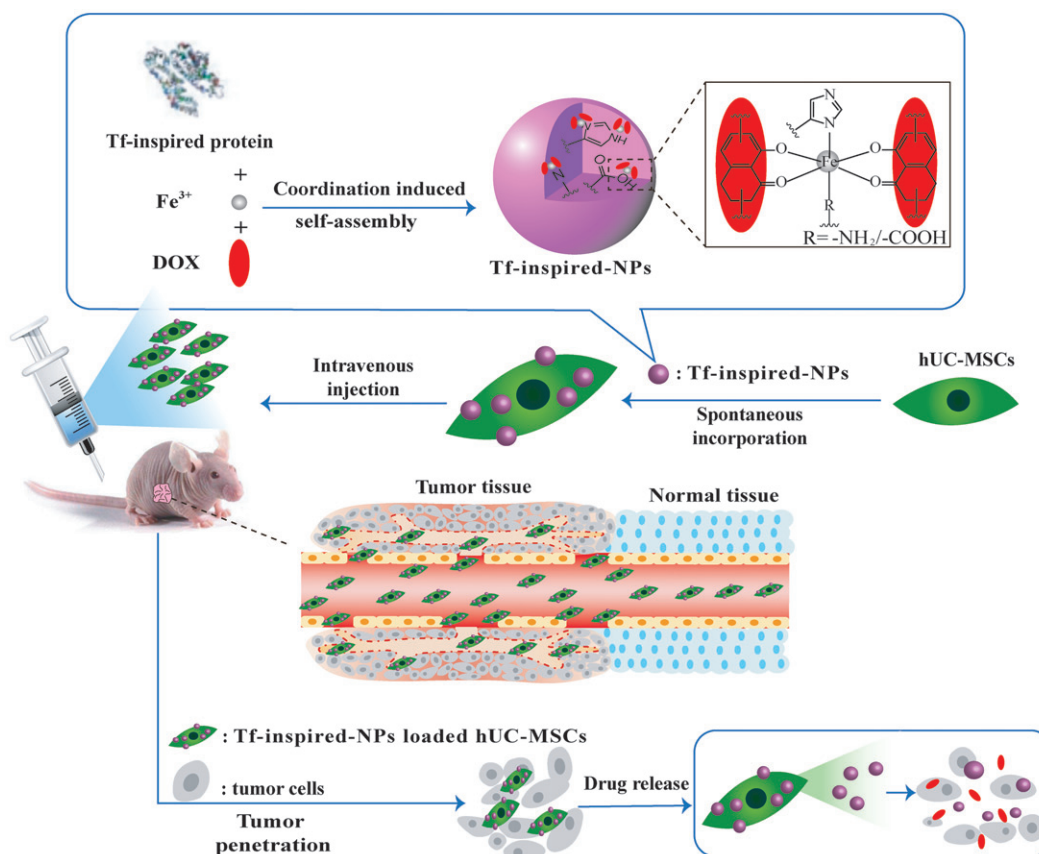
Most cancer therapeutic solutions are concerned to surgical techniques and chemotherapy regimens, that are supposed to reduce cancer progression and tumor cell destruction, but these strategies without intended targets lead to undesirable side effects [1]. Drug delivery systems via nanoparticles (NPs) can improve the pharmacologic properties of traditional chemotherapy drugs and ameliorate the therapeutic index [2–5]. Consequently, a biomimetic drug delivery system (Tf-inspired-NPs), inspired by the pH-dependent ferric ion transport and release manner of transferrin, was previously developed for combating doxorubicin-resistant breast cancer [6]. But, the delivery system is not an active targeted process, the Tf-inspired-NPs must first accumulate passively in tumor due to the enhanced permeation and retention effect (EPR), followed by binding to tumor cells. Thus, a stronger automatic targeted delivery system is needed.

Since mesenchymal stem cells (MSCs) have many unique and therapeutically advantageous features, such as easy acquisition, low immunogenicity, fast *ex vivo* expansion and feasibility of autologous transplantation [7], inherent tumor-tropic and migratory properties [8], which make them ideal vehicles for targeted drug delivery system.

Over the past few years, MSCs have been genetically modified to express anti-tumor cytokines such as interleukin-2 (IL-2) [9], IL-12 [10] and interferon β (IFN- β) [11], which have shown to inhibit the growth of melanoma, breast and hepatoma tumors. But the genes contained in MSCs caused

self-damage because of toxicity, immunogenicity or insertional mutagenesis. MSCs have also been extensively investigated as carriers of chemotherapy drugs including 5-fluorouracil [12], doxorubicin [13,14] and paclitaxel [15], these studies has made a distinguished attempt to build a new targeted drug delivery system and provided vast experience. However, there remain several problems that cannot be ignored. First, un-encapsulated drugs have cytotoxicity against MSCs, destructing the intrinsic cell functions and further reducing the tumor tracking efficiency [16]; Next, MSCs can reject internalized drugs and excrete free drugs by over-expressed transmembrane efflux pumps, which will hamper the intracellular accumulation of small molecules [17]. Besides that, when approach the tumor cell membrane, free drug are not able to accumulate in the tumor due to the lack of targeted surface groups [18].

So we hypothesize that without changing the cell status and viability, combining NPs and MSCs directly by auto internalization will enable successful loading and retention of cytotoxic drugs to reach a tumor position. Therefore, MSCs loaded with NPs will be capable to actively accumulate at tumor and slowly release its therapeutic contains, which could result in effective inhibition of tumor growth. We uploaded a doxorubicin-transferrin-inspired drug delivery system (Tf-inspired-NPs) to human umbilical cord mesenchymal stem cells (hUC-MSCs) for tumor-tropic therapy. Tf-inspired-NPs were prepared via environment-friendly method and were well redisposed in saline solution after lyophilization [6]. Tf-inspired-NPs loaded hUC-MSCs showed no significant



Scheme 1. hUC-MSCs-Tf-inspired-NPs transport process, consists of spontaneous incubation of Tf-inspired NPs and hUC-MSCs. After *in vivo* injection, loaded hUC-MSCs migrate to tumor cells and exhibit tumor specificity and then release their original form of complex or free DOX.

adverse effect on cell proliferation, viability and tropic ability towards MCF-7 human breast cancer cells. The obtained time bombs of hUC-MSCs-Tf-inspired-NPs effectively migrated towards the MCF-7 xenograft, which showed more extensive and prolonged drug accumulation at tumor tissues, and further actually promoted tumor-cell apoptosis compared with free drug or the drug-loaded Tf-inspired-NPs (Scheme 1). With extraordinarily high cargo capacity of Tf-inspired-NPs and vigorous tumor-tropic ability of hUC-MSCs, nano-loaded hUC-MSCs will prospectively provide an attractive foreground for targeted tumor therapy.

Materials and methods

Cells and animals

Human umbilical cords were obtained from healthy women (all patients signed informed consent to participate in the study and this work was approved by the Jiangsu Province People's Hospital for Women's and Children's Department, China). Female BALB/c nude mice, 6–8 weeks old, 18–22 g weight, were supplied by Yangzhou University Comparative Medical Center (Jiangsu, China) and kept under specific pathogen-free conditions.

Isolation and culture of hUC-MSCs

All procedures were conducted in accordance with the guidelines of the Medical Ethics Committee of the Health Bureau.

Blood vessels separated from umbilical cord were isolated and cut into 1 mm³ on a cold dish, followed by 1.5 h digestion in 1 mg/mL collagenase IV (Biosharp, Anhui, China) at 37 °C to obtain single cell suspension. The suspension was centrifuged at 2000 rpm for 5 min and then planted in a 100 mm dish with Dulbecco's modified Eagle's medium which included 10% FBS, 100 mM non-essential amino acids, 100 mM sodium pyruvate, 55 mM β-mercaptoethanol, 200 mM L-glutamine, 20 μg/mL EGF, 100 IU/mL penicillin and 100 μg/mL streptomycin (All from Gibco, Carlsbad, CA). Later, hUC-MSCs were incubated at 37 °C, 5% CO₂ for ~10 days. When cells reached 70–80% confluences, they were harvested with 0.05% trypsin (Gibco) and subcultured with the same medium. All experiments were performed within the fifth passage of hUC-MSCs.

Characterization of hUC-MSCs

The International Society for Cellular Therapy (ISCT) has defined that the MSCs can express the surface markers CD29, CD44, CD73, CD90 but lack of expression of CD34, CD45, CD11b [19,20]. hUC-MSCs at the third passage were trypsinized and washed twice with PBS and every 1 × 10⁵ cells were stained separately by human monoclonal antibodies CD44-FITC, CD90-FITC, CD45-FITC and CD11b-FITC (BD Biosciences, Franklin Lakes, NJ) at 4 °C in the dark for 20 min, concomitantly with fluorescein isothiocyanate (FITC) isotype as control. Then the cells were washed and suspended in

Table 1. Forward and reverse primer sequences used for reverse transcriptase PCR.

Gene	Forward primer	Reverse primer
CD34 [35]	CTACAACACCTAGTACCCTTGGA	GGTGAACACTGTGCTGATTACA
CD90 [39]	ATCGCTCTCCTGTAACAGC	CTCGTACTGGATGGGTGAAC
CD44 [37]	GGCAGGCCACCTACAAGAG	CATTGTGGGCAAGGTGCTATT
CD45 [38]	ACCACAAGTTTACTAACGCAAGT	TTTGAGGGGGATTCCAGGTAAT
CD11b [40]	ACTGGTGAAGCCAATAACGCA	TCCGTGATGACAAGTACGATCTT
CD29 [34]	CCTACTTCTGCACGATGTGATG	CCTTGTACTACGGTTGGTTACATT
CD73 [36]	CCAGTACCAGGGCACTATCTG	TGGCTCGATCAGTCTTCCA

500 μ L of FACS buffer and analyzed by Flow Cytometer (Accuri C6, BD Biosciences).

Besides the markers defined by the ISCT, additional surface markers were detected by Real-time polymerase chain reaction (PCR) to confirm the results. Total RNA was extracted by trizol according to kit instructions (Ambion, Foster City, CA). Then cDNA was prepared by All-In-One RT MasterMix (ABM). Forward and reverse primer sequences used in reverse transcriptase PCR (Table 1) were designed by a software Primer 5.0 (PREMIER Biosoft International, Palo Alto, CA), according to the mRNA information of each gene obtained from National Center for Biotechnology Information (NCBI) database. Then real-time PCR was performed using EvaGreen 2 \times qPCR MasterMix (ABM) on Light Cycler 480 II (Roche Diagnostics, Basel, Switzerland) by forward and reverse primers.

On the other hand, to determine a multiple differentiation potentiality of hUC-MSCs, three different induction experiments were utilized. We performed adipogenic, osteogenic and chondrogenic differentiation using the Human Mesenchymal Stem Cell Functional Identification Kit (R&D Systems Inc., Minneapolis, MN). The induction processes of the three lineages were performed according to the manufacturer's instructions. The differentiation media was changed every two days. After 10 days, the adipogenic, osteogenic and chondrogenic differentiation were tested by oil red staining, Alizarin Red-S staining and alcian 8GX blue staining (Sigma-Aldrich, St. Louis, MO).

Preparation and characterization of Tf-inspired-NPs

In order to make encapsulated drug release rapidly in the acidic environment of tumor cells, we designed a pH-responsive biomimetic drug delivery system Tf-inspired-NPs based on the principle that transferrin can transports iron ions in the body and respond to pH in specific cells to release iron ions.

For the synthesis of Tf-inspired protein, bovine serum albumin (BSA, 25 g, 0.368 mmol, Mw = 6.8 KDa, Biosharp, China) and Histamine hydrochloride (HA, 13.875 g, 75.379 mmol, Chemlin, China) were dissolved in 50 ml of phosphate buffer saline (PBS; pH 7.4), later the pH value was adjusted to 4.75 with a pH meter (Ohaus, Parsippany, NJ). 1-Ethyl-3-(3-dimethylaminopropyl) carbodiimide hydrochloride (EDC-HCl; 4.5 g, 23.474 mmol) was added to the resultant solution by stirring the mixture at room temperature for 6 h. The reaction was terminated by the addition of an acetate buffer (16.25 mL, 4 M and pH 4.75). The solution was adequately dialyzed against deionized water by dialysis bag

(molecular weight cut-off MWCO = 14 K, Baomanbio, China) and was finally lyophilized.

To prepare Tf-inspired-NPs, ferric ions and DOX were mixed in the certain mole ratio and were added to 1% (w/v) Tf-inspired protein aqueous solution dropwise. The resulting solution was stirred for 30 min at room temperature after adjusting the pH to 7.4. The uncoordinated DOX was removed by dialysis bag for 6 h. Ultimately, purple-colored Tf-inspired NPs powder containing DOX-Fe³⁺ complexes were obtained after lyophilization. An empty carrier (Tf-inspired protein/Fe³⁺) was also prepared by the same method without DOX addition.

We characterized Tf-inspired-NPs through the particle size and morphology. The size distribution of Tf-inspired-NPs in deionized water was determined by Zeta Plus particle size analyzer (Brookhaven Instruments, Holtsville, NY) and the morphology was examined by scanning electron microscope (SEM, Hitachi, S-4800, Shiga, Japan).

Cytotoxicity of drug on hUC-MSCs

To evaluate the cytotoxicity of DOX (Beijing Huafeng United Technology, China), Tf-inspired protein/Fe³⁺ and Tf-inspired-NPs on hUC-MSCs (3-(4,5-dimethylthiazol-2-yl)-2,5-diphenyltetrazolium bromide) tetrazolium reduction (MTT) assay was used, 5 \times 10⁴ hUC-MSCs/well were seeded into 96-well plates and incubated at 37 °C and 5% CO₂ for 24 h. When cells reached 70–80% confluence, the medium was replaced with DOX, Tf-inspired protein/Fe³⁺ and Tf-inspired-NPs at different concentrations and were re-incubated for 6 h. The medium was then replaced with 200 μ L fresh serum-free medium containing 0.5 mg/mL MTT (KeyGEN Biotech, Nanjing, China) for 2 h. Later, the medium was replaced by 100 μ L dimethyl sulfoxide (DMSO; Tianjin Concord, China) and the color was measured at 570 nm by microplate reader (Bio-Tek, Winooski, VT). For proliferation experiments, 5 \times 10³ hUC-MSCs/well were treated with 50 μ g/mL DOX and Tf-inspired-NPs (DOX-equiv). Later viability of cells was tested after incubation for 1, 3 and 5 days. Cell proliferation was determined by MTT assay. Data were expressed as mean \pm standard deviation (SD) of at least three independent experiments.

Uptake of Tf-inspired-NPs by hUC-MSCs

To determine the optimal incubation time, 1 \times 10⁵ hUC-MSCs cells were incubated in PBS mixed with 25 μ g/mL DOX and Tf-inspired-NPs (DOX-equiv) for 2, 4, 6, 8, 10, 12, 24 and 48 h, respectively. Later the cells were washed twice with PBS and tested by a Flow Cytometer (FACS Calibur, BD Biosciences) in the FL-2 channel, depending on the red fluorescence of DOX. Besides that, to study the drug concentration effect on the uptake intensity, DOX and Tf-inspired-NPs were tested at different concentrations ranging from 10–100 μ g/mL. These drugs were incubated with 1 \times 10⁵ hUC-MSCs at 37 °C for 6 h and were determined by a Flow Cytometer.

Quantitative determination of drug loading content in hUC-MSCs

The hUC-MSCs system were constructed by co-incubation of 5×10^5 hUC-MSCs with 50 $\mu\text{g/mL}$ DOX and Tf-inspired-NPs (DOX-equiv) for 6 h. The total DOX content of loaded hUC-MSCs were determined by high performance liquid chromatography (HPLC) (LC-2010C, Japan) with the concentration ranging from 0.1 to 10 $\mu\text{g/mL}$. After the cells were washed and counted, 200 μL of cell lysis buffer was added to obtain cell lysates. Later the lysate was extracted by vortex extraction with 800 μL of methanol at 12,000 rpm for 5 min. Then, the DOX content of the supernatant was separated by HPLC using fluorescence detection ($\lambda_{\text{ex}} = 480 \text{ nm}$, $\lambda_{\text{em}} = 560 \text{ nm}$; RF-20 A, Japan). Using a C18 column (Agilent) with a mobile phase of 0.01 mol/l KH_2PO_4 : methanol: acetic acid = 40: 60: 0.4 (v/v/v).

Drug release from drug loaded hUC-MSCs

To evaluate drug release efficacy, hUC-MSCs were incubated with 50 $\mu\text{g/mL}$ DOX and Tf-inspired-NPs (DOX-equiv) for 6 h. At the end of drug priming, the cells were washed, trypsinized and transferred to a new flask at a density of 5×10^5 hUC-MSCs/well and were incubated at 37 °C for 0.5, 1, 4, 6, 24 and 48 h. Later the cells were collected and centrifuged at 300 g for 5 min and 600 μL supernatant was used to test the percent of drug release from loaded hUC-MSCs. The drug release was calculated for each time point and was plotted by measuring absorbance at 480 nm Using Equation (1).

$$\begin{aligned} & \text{Cumulative DOX released (\%)} \\ & = \text{Amount of released DOX/Amount of total DOX in hUC} \\ & \quad \text{MSCs} \times 100 \end{aligned} \quad (1)$$

To confirm that the released DOX was encapsulated mainly in Tf-inspired-NPs, the supernatant was obtained was centrifugated at 14,000 g for 15 min by a centrifugal filter device (10K MWCO, Millipore, Billerica, MA). The amount of free DOX (Q_F) in the filtrate was determined by HPLC. The ratio of the encapsulated DOX (Q_E) to the total released DOX (Q_S) in the supernatant was calculated by using the formula ($Q_E = (Q_S - Q_F)/Q_S \times 100\%$) [21]. For morphology observation, the supernatant was freeze-dried at -80°C and was examined by SEM after coating it with gold-palladium [22].

In vitro migration of hUC-MSCs

To assess migration capability of hUC-MSCs, cell migration experiments were performed using 24-well transwell plate (PET membrane 8 μm pore sizes, Corning Incorporated Costar, Corning, NY). In 200 μL serum-free medium, 2×10^5 unloaded and loaded hUC-MSCs were suspended and seeded in the upper well of the transwell chambers, individually. In each group, one bottom was filled with 600 μL 0.5% serum medium as control, and the other bottom was filled with 4×10^5 MCF-7 cells suspended in the same medium. After 24 h incubation, the cells that did not migrate through the pores were removed with a cotton swab. The cells on the lower surface of the membrane were then fixed in methanol for 30 min and stained with 0.1% crystal violet for 20 min.

Thereafter, each sample was observed by fluorescence inverted microscope (Olympus, Tokyo, Japan) and 10 photographs were captured in a 10-fold objective lens to count the number of stained cells migrating through the membrane pore.

Subcutaneous MCF-7 breast cancer model

For *in vivo* efficacy determination and *in vivo* imaging, 1.5 mg/kg estradiol (Shanghai Aladdin Bio-Chem Technology Co. Ltd, Shanghai, China) was injected into the muscle of nude mice. Later 1×10^7 cells in 100 μL PBS of MCF-7 cell line were injected into the mice armpit subcutaneously. Tumor size of challenged mice were measured by a caliper and thereafter the tumor volume was calculated using Equation (2)

$$\text{Tumor volume} = (\text{tumor length}) \times (\text{tumor width})^2 / 2$$

In vivo distribution of hUC-MSCs

To examine the distribution of hUC-MSCs *in vivo*, DiR (Shanghai Jingke, China) was used as a fluorescent probe to label hUC-MSCs. Tumor bearing mice were injected intravenously with 1×10^6 cells/200 μL hUC-MSCs-DiR as an experimental group and the PBS solution was used as the control group. After 24 h, mice were anesthetized by intraperitoneal injection of 10% chloral hydrate (4 ml/kg body weight). The tumor accumulation and distribution of hUC-MSCs were recorded using an *in vivo* imaging system (FXPRO, Kodak, Rochester, NY) with a DiR filter set at excitation, 790 nm and emission, 720/min, respectively.

In vivo anti- MCF-7 tumor cells effect

When the tumor sizes of nude mice bearing subcutaneous MCF-7 breast cancer reached $\sim 100 \text{ mm}^3$, to evaluate antitumor efficacy, they were randomly divided into five groups ($n=6$): control group (Saline), hUC-MSCs group (hUC-MSCs), DOX group (DOX), Tf-inspired-NPs group (Tf-inspired-NPs) and hUC-MSCs-Tf-inspired-NPs group (hUC-MSCs-Tf-inspired-NPs). All samples were injected via tail veins with 2.5 mg/kg every four days. Tumor volume was measured daily with a caliper.

Histology and cell apoptosis

After the mice were sacrificed, tumor mass and cells of heart, liver, spleen, lung and kidney were detected by hematoxylin and eosin (H&E) staining and terminal deoxynucleotidyl transferase dUTP nick end labeling (TUNEL). The tumor samples were fixed in 40% formalin and were made into 5 mm thick paraffin sections on which HE staining were performed. Immunofluorescence of tumor tissue was treated with TUNEL assay kit (Roche) for labeling apoptotic cells, using the Equation (3).

$$\text{Apoptosisrate (\%)} = \text{IOD/Area} \times 100\% \quad (3)$$

Statistical analysis

Statistical analysis was performed using the Graphpad Prism 6.0 software (GraphPad Software, La Jolla, CA) and at least three independent experiments were carried out. The sample size was not predetermined using statistical methods. The nude mice were randomized to different groups before the treatment, but the outcome assessment and data analysis were not blinded. All the data were presented as mean \pm SD and comparison among the different groups was performed by one-way analysis of variance (ANOVA) and student's *t*-test was used to analyze the data. Statistical significance was set at **p* < .05, ***p* < .01 and ****p* < .001.

Results

Design of the targeted delivery system hUC-MSCs-Tf-inspired-NPs

This paper further enhanced the anti-tumor effects of Tf-inspired-NPs by hUC-MSCs. *In vivo* imaging showed that Tf-inspired-NPs mainly accumulated in the tumor site through the EPR effect, with some nanoparticles remaining in liver, but almost all hUC-MSCs-Tf-inspired-NPs gathered in the tumor site, increasing the anti-tumor efficacy and reducing the side effects. Anti-tumor experiment of hUC-MSCs-Tf-inspired-NPs group exhibited more extensive permeability and enhanced apoptosis of tumor cells than that of Tf-inspired NPs. As a cell-based therapy, without additional genetic manipulation or chemical modification, the new model hUC-MSCs-Tf-inspired-NPs can have more application prospects.

Characterization of hUC-MSCs and Tf-inspired-NPs

We characterized hUC-MSCs through their morphological and physiological criteria. The microscopic examination of adherent cells showed a fibroblast-like morphology and these cells were almost homogeneous, resembling MSC morphology (Figure 1(a)). Furthermore, these cells exhibit all the MSC characteristics defined by the ISCT. Firstly, they were plastic adherent. Secondly, we investigated the surface markers of isolated hUC-MSCs by using Flow cytometer and qPCR. As showed in Figure 1(b,c), the isolated cells expressed low percentage of CD11b, CD45 and CD34, while they showed high expression of MSC markers: CD44, CD29, CD73 and CD90. These results indicate a relatively homogeneous mesenchymal phenotypic population of hUC-MSCs. To further confirm the MSCs identity of isolated cells, we examined the differentiation potential of these cells towards mesenchymal lineages. As showed in Figure 1(d-i), these hUC-MSCs exhibit adipogenic, osteogenic and osteogenic differentiation potential when compared with the control undifferentiated cells, detected by oil red staining, Alizarin Red-S staining and alcian 8GX blue staining, respectively.

SEM image showed that Tf-inspired NPs were nanometer-sized vehicles (Figure 1(j)) and the average diameter determined by dynamic light scattering (DLS) technique (Zeta Plus particle size analyzer) was 78 nm (Figure 1(k)).

hUC-MSCs sensitivity to DOX, Tf-inspired protein/Fe³⁺ and Tf-inspired-NPs

To test the sensitivity of hUC-MSCs to DOX, Tf-inspired protein/Fe³⁺ and Tf-inspired-NPs, cell survival was assessed by cytotoxicity at 6 h and anti-proliferation at five days. As showed in Figure 2(a-c), DOX, Tf-inspired protein/Fe³⁺ and Tf-inspired-NPs did not show significant cytotoxicity to hUC-MSCs. Even at a high concentrations of DOX (200 μ g/mL), hUC-MSCs remained highly viability in DOX (90%) and Tf-inspired-NPs (97%), which indicated that, there is no difference between hUC-MSCs survival incubated with free DOX and that with its complex for 6 h. Anti-proliferation of hUC-MSCs was induced by three drugs at different levels (Figure 2(d)). In the first 3 days, some hUC-MSCs died at Tf-inspired-NPs. However, five days post NPs internalization, the viability of hUC-MSCs increased significantly, which suggested that prolonged incubation of Tf-inspired-NPs was not toxic to hUC-MSCs, but only delayed its proliferation. For free DOX, the proliferation experiment showed that the viability of hUC-MSCs decreased with the time prolonged. Results showed that it's necessary to incubate hUC-MSCs with Tf-inspired-NPs instead of DOX for a long time. Thus, the essential hUC-MSCs can be used for *in vivo* studies to encapsulate NPs.

hUC-MSCs uptake of Tf-inspired-NPs

Cell uptake behavior was studied at different culture time and drug concentration to explore the optimal culture conditions. As showed in Figure 3(a), cell uptake showed a time-dependent manner at the same drug dose (25 μ g/mL, DOX equiv). For detection of DOX and Tf-inspired-NPs, the uptake of the complex increased significantly with the increasing time, but no significant change was observed after 6 h, indicating that the optimal time of cells uptake is approximately 6 h. On the other hand, the investigation of different concentrations showed that the uptake behavior of DOX increased gradually with the increasing drug dose, while Tf-inspired-NPs represented no significant statistical difference between 50 and 100 μ g/mL (DOX-equiv; Figure 3(b)). Thus, the optimal drug loading conditions, that can maximize the drug loading content, are incubating hUC-MSCs with Tf-inspired-NPs at the concentration of 50 μ g/mL (DOX equiv) for 6 h.

Drug loading content in hUC-MSCs

To assess drug loading content, loaded hUC-MSCs was determined by HPLC. After incubating with 50 μ g/mL DOX or Tf-inspired-NPs for 6 h, 1×10^5 drug loaded hUC-MSCs were extracted for analysis. As presented in the Figure 4(a), DOX and Tf-inspired NPs have an average DOX content of 22.31 and 20.08 pg/cell, respectively.

Drug release from loaded hUC-MSCs

To estimate the release of equivalent content of DOX and Tf-inspired-NPs from loaded hUC-MSCs at certain time points, hUC-MSCs was loaded with DOX and Tf-inspired-NPs (50 μ g/mL, DOX-equiv), later the culture supernatant was

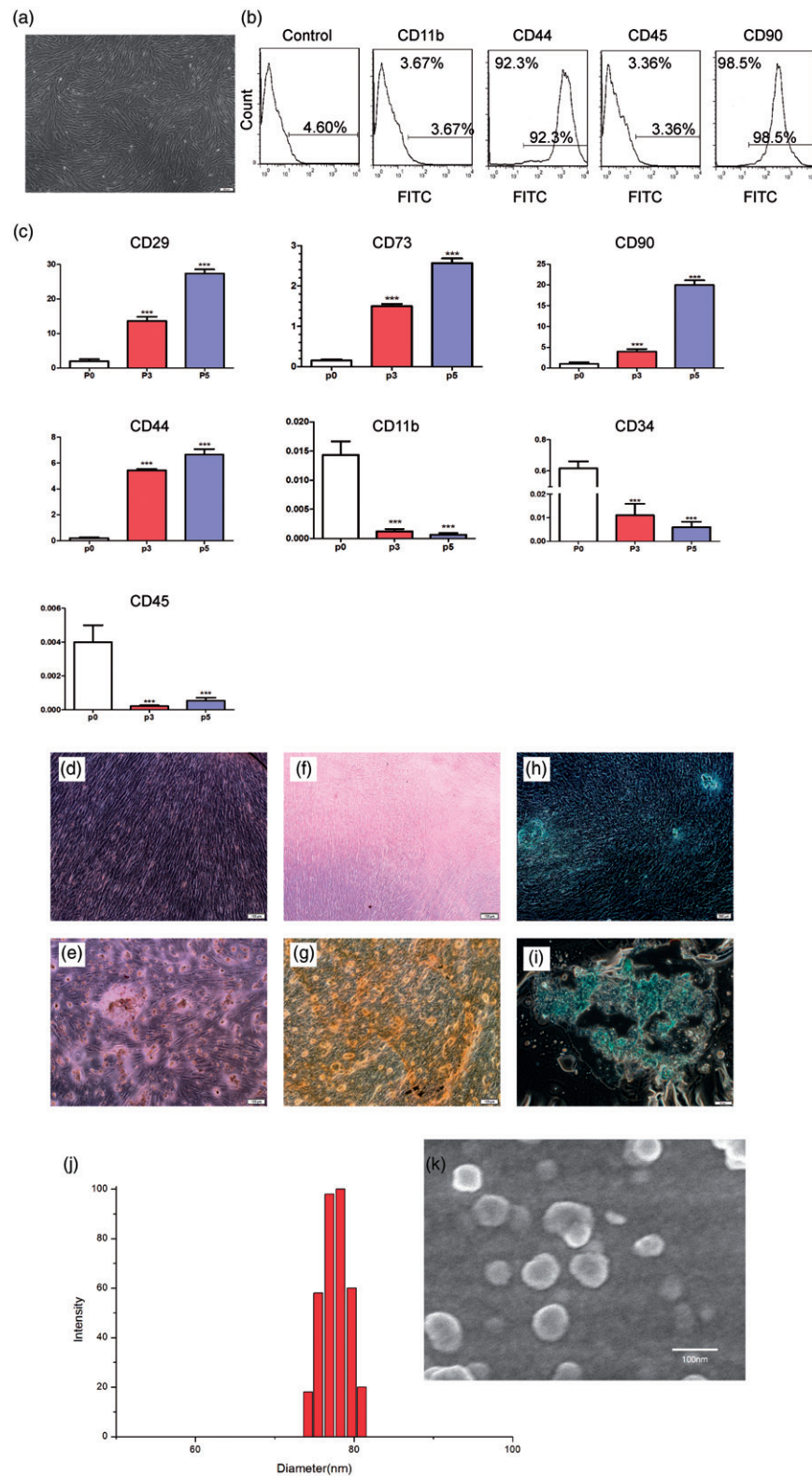


Figure 1. Characterization of hUC-MSCs. (a) Phase-contrast image of isolated hUC-MSCs (passage 3) showing homogeneous fibroblast-like cells. Magnification: 10 \times ; scale bar = 100 μ m. (b) Immunophenotyping for isolated hUC-MSCs; cells were labeled with FITC and examined by flow cytometer. The immunophenotyping profile of hUC-MSCs showed negative for CD34 and CD11b but positive for CD44 and CD90. (c) mRNA expression in different hUC-MSCs populations (p0, p3 and p5) by real-time PCR (***) $p < .001$ compared to the control. (d–i) Successfully differentiated into adipocytes (stained red with Oil Red), osteoblasts (stained with Alizarin Red) and chondrocyte (stained with Alcian 8GX blue Alizarin Red) cells. Scale bar = 100 μ m. (j) Scanning electron microscopy (SEM) image of Tf-inspired-NPs. (k) Histogram of particle-size distribution of Tf-inspired-NPs obtained by dynamic light scattering measurements (DLS).

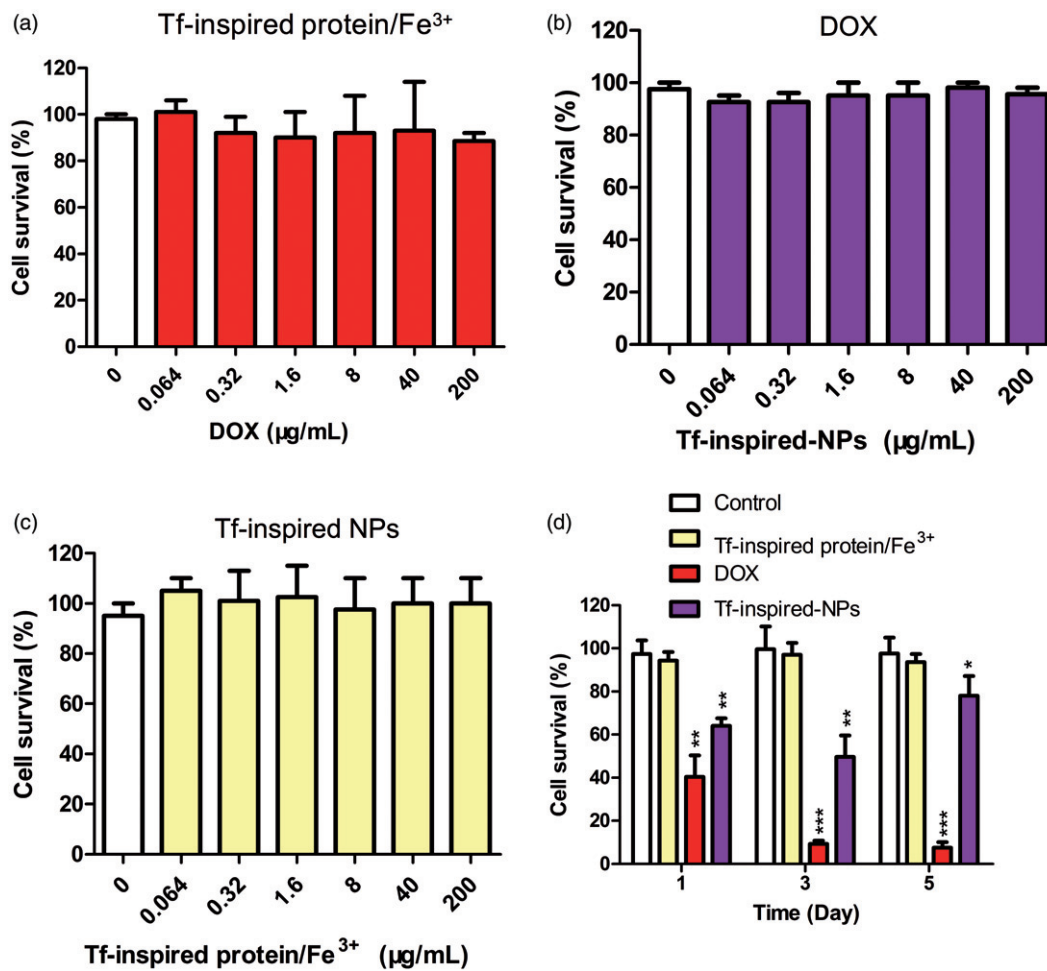


Figure 2. Influence of the drugs on hUC-MSCs cells viability. hUC-MSCs were co-cultured with Tf-inspired-NPs (a), DOX (b) and Tf-inspired protein/Fe³⁺ (c) for 6 h to investigate cytotoxicity. Influence of the drugs uptake on hUC-MSCs cell survival (d). hUC-MSCs were incubated at 37 °C with 50 µg/mL DOX, Tf-inspired protein/Fe³⁺ and Tf-inspired-NPs. After 1, 3 and 5 days, cell survival was determined. Viability of the control group receiving none drugs was considered as 100%. Data were expressed as mean ± standard deviation ($n = 3$). * $p < .05$, ** $p < .01$ and *** $p < .001$.

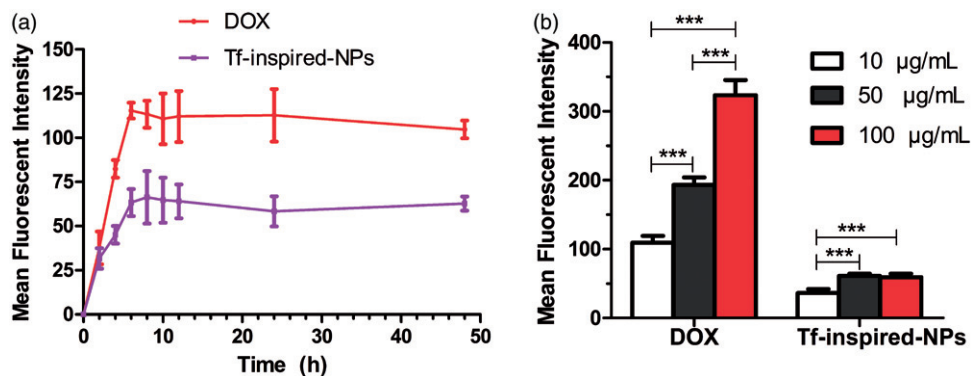


Figure 3. Total cellular uptake of free DOX and Tf-inspired-NPs by hUC-MSCs. (a) Depicts the incubation time-dependent manner of hUC-MSCs uptake; (b) Reports the mean fluorescence intensity of DOX and Tf-inspired-NPs under different drug concentration. Data is expressed as mean ± standard deviation ($n = 3$), *** $p < .001$.

tested at different time points. As showed in Figure 4(b), the release rate of hUC-MSCs-DOX was higher than those of hUC-MSCs-Tf-inspired-NPs. hUC-MSCs-Tf-inspired-NPs only released 20% of the drug in the first 3 h and then sustainably released about 55% within 24 h. We found that the release of DOX from hUC-MSCs during 48 h was significantly higher than that of Tf-inspired-NPs ($p < .05$), which could be ascribed to the passive diffusion of a small molecule. Quantitative analysis

and characterization of Tf-inspired-NPs in hUC-MSCs showed about 85% of the DOX released from hUC-MSCs was encapsulated in Tf-inspired-NPs (Figure 4(c)).

In vitro tumor tropism of hUC-MSCs

To evaluate tumor tendency migration of hUC-MSCs-Tf-inspired-NPs, the migration of unloaded and loaded hUC-

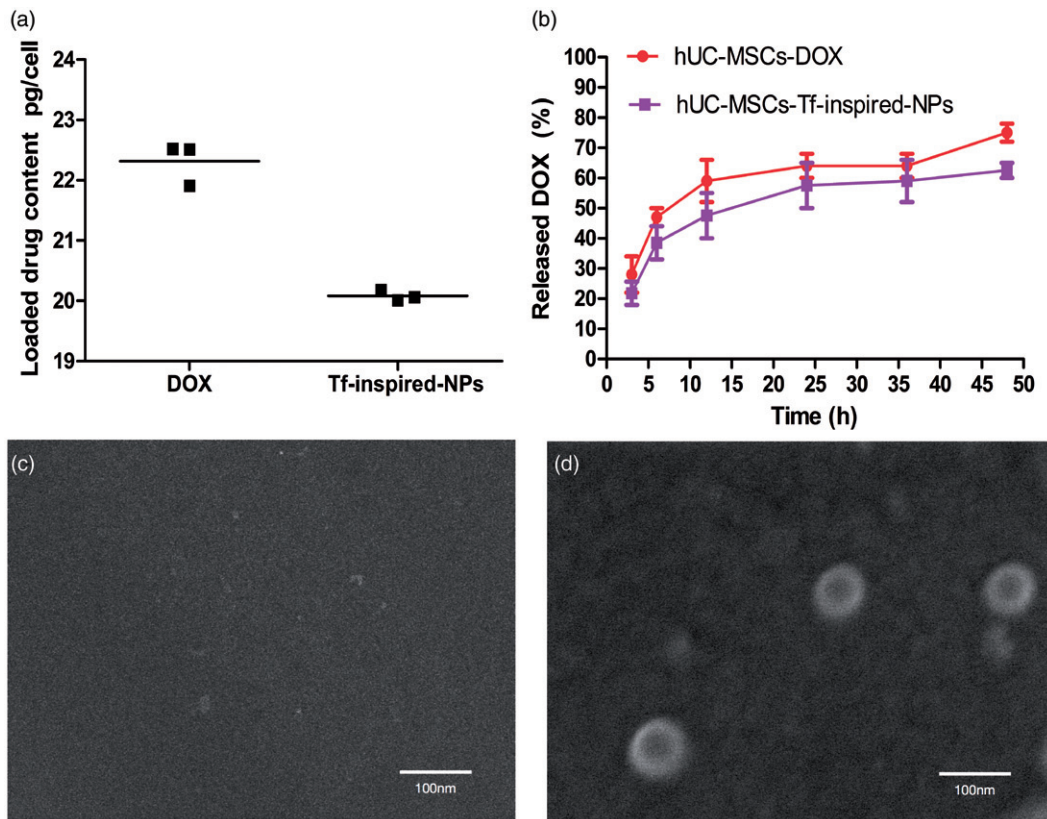


Figure 4. Drug loading (a) and *in vitro* release (b) of doxorubicin from hUC-MSCs-DOX and hUC-MSCs-Tf-inspired-NPs. SEM images of the supernatant of hUC-MSCs-DOX (c) and hUC-MSCs-Tf-inspired-NPs (d) post 6 h culturing. Data was expressed as mean \pm standard deviation ($n = 3$), * $p < .05$.

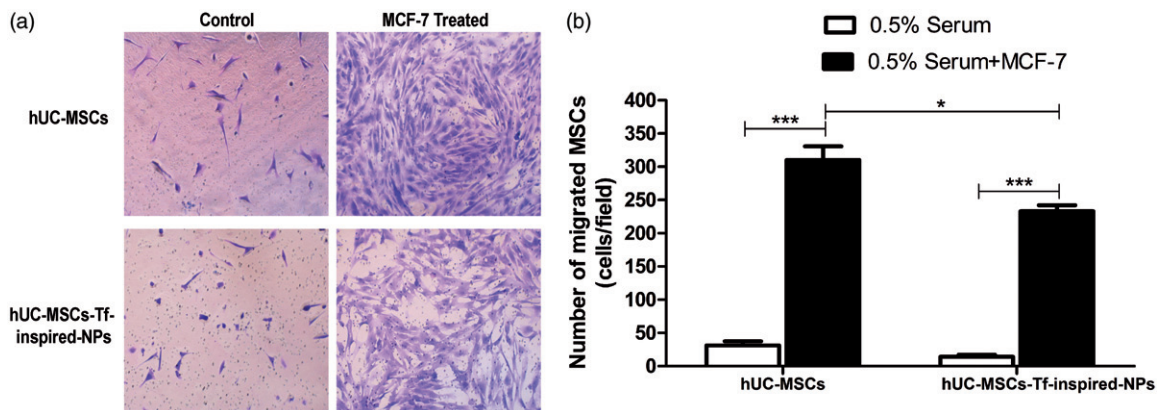


Figure 5. (a) Impact of uploading drug on hUC-MSCs migration. Typical photos of loaded and unloaded hUC-MSCs migration through the membrane pores; (b) OD₅₇₀ value of stain crystal violet in each group. 0.5% serum was used as control group. Data were presented as mean \pm standard deviation, ($n = 6$ replicates for each group), * $p < .05$, ** $p < .01$, *** $p < .001$.

MSCs through the membrane pore to MCF-7 cells which were in the bottom chamber was tested. As showed in Figure 5, the migration of loaded hUC-MSCs to MCF-7 cells presented a statistical significant reduction in the number of cells compared to unloaded ones ($p < .05$), but it still showed a significant increase in comparison with the control group ($p < .001$). Results indicated the tumor tropism of hUC-MSCs-Tf-inspired-NPs and their suitability for drug delivery.

In vivo distribution of hUC-MSCs

To prove *in vivo* tumor tendency of hUC-MSCs, DiR was utilized as the near infrared fluorescent probe. As presented in

Figure 6(a), hUC-MSCs-DiR were mainly targeted to tumor and the fluorescence was detectable even 24 h post systemic injection. The tracking signals in tumor, heart, liver, spleen, lung, kidney and pancreas showed that, large amount of hUC-MSCs-DiR accumulated in the tumor, small amount accumulated in liver and lung and almost none accumulated in other organs (Figure 6(b)). This demonstrated the *in vivo* tumor homing and penetrative potential of hUC-MSCs.

In vivo anti-tumor efficacy of loaded hUC-MSCs

In order to assess an *in vivo* antitumor efficacy of loaded hUC-MSCs, female BALB/c nude mice model were challenged

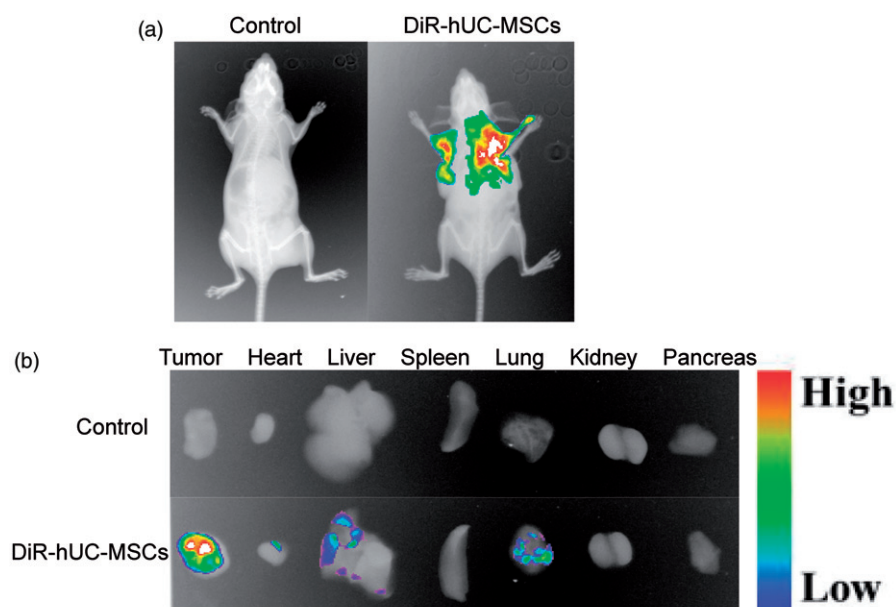


Figure 6. *In vivo* distribution of DiR-hUC-MSCs. (a) *In vivo* images (side view) of mice bearing MCF-7 tumors at 24 h after DiR-hUC-MSCs injection. (b) *Ex vivo* images of tumors and major organs at 24 h after hUC-MSCs injection.

by MCF-7 cell line, and were treated as described above. Results showed that, tumors of mice treated with saline or hUC-MSCs grew rapidly (Figure 7(a)), while those treated with free DOX and Tf-inspired-NPs moderately slowed tumor growth. However, tumor volume and size data showed that mice treated with hUC-MSCs-Tf-inspired-NPs significantly inhibited tumor growth (Figure 7(b,c)). To further assess the relative toxicity of different treatments, H & E staining and TUNEL methods was used. The apoptosis of tumor cells in mice treated by hUC-MSCs-Tf-inspired-NPs was found to be more severe than that of free DOX or Tf-inspired-NPs treatment group (Figure 7(d,e)). The integrated optical density (IOD) of TUNEL stained area in hUC-MSCs-Tf-inspired-NPs group was significantly higher than that in free DOX or Tf-inspired-NPs group, which indicated that hUC-MSCs-Tf-inspired-NPs showed high potential anti-tumor activity.

Discussion

The targeted delivery of anticancer agents is a promising field in anticancer therapy. Over the past few decades, various NPs provided versatile strategies for the tropic therapy of tumor [23–26]. However, most nano-medicine including those decorated with specific binding ligands could just accumulate passively in tumor tissues via EPR effect [27,28] and only few fractions could accumulate in tumor tissues and effect tumor cells, which would be insufficient for a successful therapy [29,30].

MSCs have inherent tumor tropic and migratory properties which can be used as an efficient drug delivery vehicles for tumor-tropic therapy [31]. Here, we particularly concentrated on MSCs derived from human umbilical cord. On incubating 50 $\mu\text{g}/\text{mL}$ (DOX equiv) with Tf-inspired-NPs at the optimal concentration for 6 h, the majority of hUC-MSCs was remain viable to perform stem properties, but limited to proliferate, which fits the precondition of fabrication and criteria of

in vivo safety. The drug loaded in hUC-MSCs-Tf-inspired-NPs group was 20.08 pg/cell approximately, showing a significantly accumulation in tumor and inhibition of tumor growth.

Reportedly, MSCs are first drawn to $\text{TNF-}\alpha$, $\text{TGF-}\beta$ and other cytokines secreted in tumor microenvironment and later drawn towards the tumor tissue [32,33]. Even though the migratory capacities of hUC-MSCs-Tf-inspired-NPs were slightly affected but they were still able to retain the tumor homing nature (Figure 5). This can be attributed to NPs attaching to the membrane of hUC-MSCs or inside hUC-MSCs, which hampered their deformation to migrate through transwell membrane. *In vivo* cancer homing effect of hUC-MSCs showed that, hUC-MSCs-DiR penetrated into the solid tumors with only a small amount accumulating in the liver and lung (Figure 6(b)).

The P-glycoprotein (P-gp) system quickly pumped out the free DOX in the cells retaining only the Tf-inspired-NPs in hUC-MSCs as drug depots for extended periods. *In vivo* anti-tumor efficiency performed on mice bearing MCF-7 breast cancer cells showed statistically that, incomparison to other groups, Tf-inspired-NPs-loaded hUC-MSCs exhibited lighter tumor volume and weight (Figure 7(a–c)) and more tumor cell apoptosis (Figure 7(d,e)). hUC-MSCs-Tf-inspired-NPs retained the tumor tropic and permeability trait of MSCs and exhibited long-term and potent anti-tumor efficacy of NPs.

Conclusions

We developed hUC-MSCs as novel targeted carrier of Tf-inspired-NPs, which have therapeutic potential to cure breast cancer. The dosage form of hUC-MSCs-Tf-inspired-NPs could dominantly accumulate in tumor tissue directly, thereby reducing the toxicity to normal tissues. In conclusion, hUC-MSCs-Tf-inspired-NPs strategy is a promising model to improve precise tumor targeting delivery.

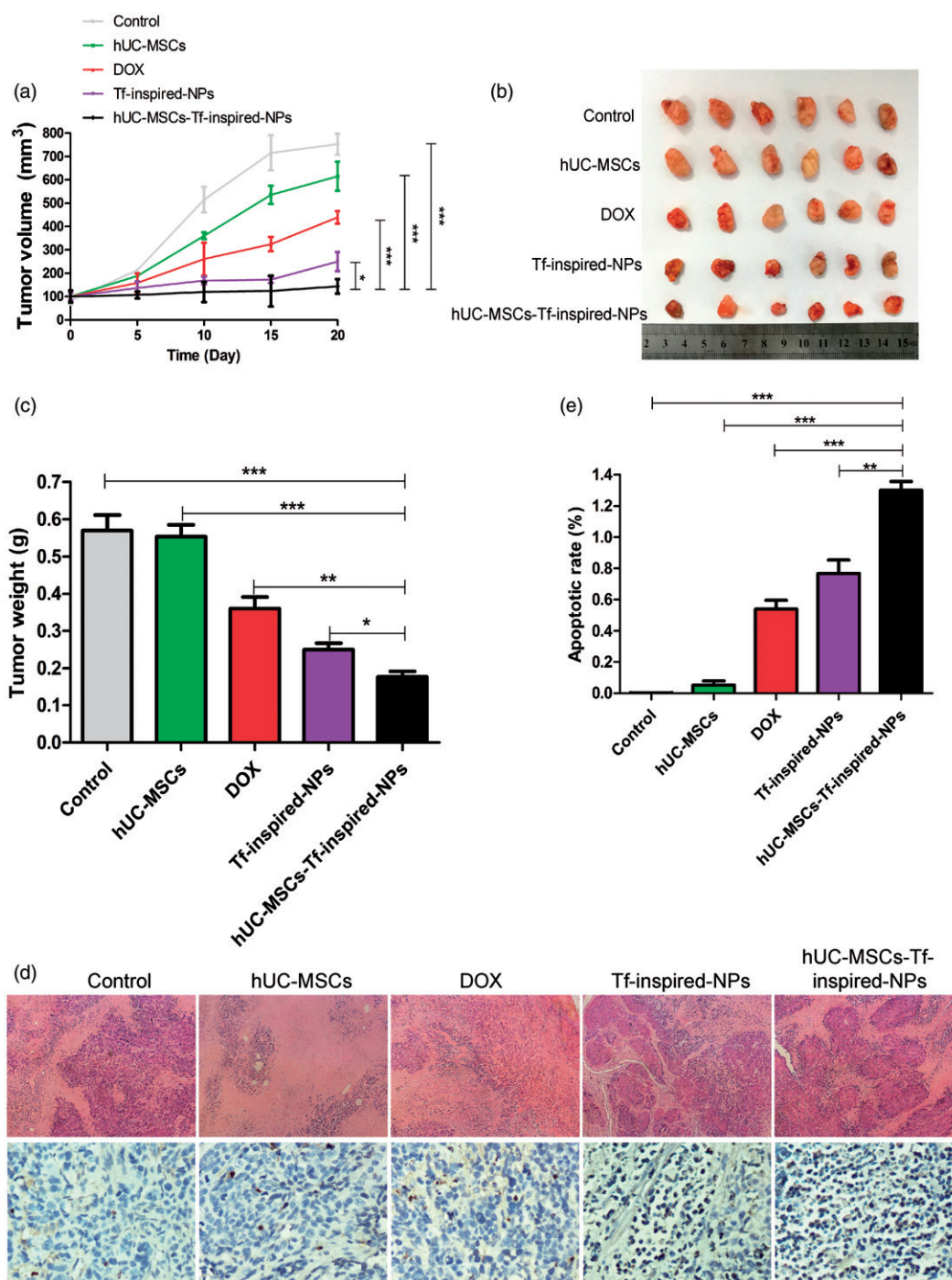


Figure 7. *In vivo* anti-tumor effects. (a) The tumor growth curves of mice after various treatments ($n = 6$, $*p < .05$, $**p < .01$, $***p < .001$). (b) Tumor tissue images and (c) tumor weights of MCF-7 bearing female BALB/c nude mice treated with different formulations after a schedule of multiple dose ($n = 6$). (d) H&E and TUNEL staining of tumor (scale bar: 100 μm). (e) Integrated optical density (IOD) value of TUNEL-position area in the section area. Mean \pm standard deviation ($n = 3$, $*p < .05$, $**p < .01$, $***p < .001$).

Disclosure statement

No potential conflict of interest was reported by the authors.

Funding

This study was funded by National Natural Science Foundation of China; National High Technology Research and Development Program of China; Top-notch Academic Programs Project of Jiangsu Higher Education Institutions; The science and technology innovation team of "Jiangsu Province Blue Project"; Jiangsu province science and technology innovation team; Excellent Youth Foundation of Jiangsu Scientific Committee

and Priority Academic Program Development of Jiangsu Higher Education Institutions (PAPD).

References

- [1] Jemal A, Bray F, Center MM, et al. Global cancer statistics. *Ca Cancer J Clin.* 2011;61:69–90.
- [2] Allen TM, Cullis PR. Drug delivery systems: entering the mainstream. *Science.* 2004;303:1818–1822.
- [3] Torchilin VP. Micellar nanocarriers: pharmaceutical perspectives. *Pharm Res.* 2007;24:1–16.

- [4] Cukierman E, Khan DR. The benefits and challenges associated with the use of drug delivery systems in cancer therapy. *Biochem Pharmacol.* 2010;80:762–770.
- [5] Kose K, Denizli A. Poly(hydroxyethyl methacrylate) based magnetic nanoparticles for lysozyme purification from chicken egg white. *Artif Cells Nanomed Biotechnol.* 2013;41:13–20.
- [6] He YJ, Xing L, Cui PF, et al. Transferrin-inspired vehicles based on pH-responsive coordination bond to combat multidrug-resistant breast cancer. *Biomaterials.* 2017;113:266–278.
- [7] Porada CD, Almeida-Porada G. Mesenchymal stem cells as therapeutics and vehicles for gene and drug delivery. *Adv Drug Deliv Rev.* 2010;62:1156–1166.
- [8] Shah K. Mesenchymal stem cells engineered for cancer therapy. *Adv Drug Deliv Rev.* 2012;64:739–748.
- [9] Nakamura K, Ito Y, Kawano Y, et al. Antitumor effect of genetically engineered mesenchymal stem cells in a rat glioma model. *Gene Ther.* 2004;11:1155–1164.
- [10] Gao P, Ding Q, Wu Z, et al. Therapeutic potential of human mesenchymal stem cells producing IL-12 in a mouse xenograft model of renal cell carcinoma. *Cancer Lett.* 2010;290:157–166.
- [11] Ling X, Marini F, Konopleva M, et al. Mesenchymal stem cells overexpressing IFN-beta inhibit breast cancer growth and metastases through Stat3 signaling in a syngeneic tumor model. *Cancer Microenviron.* 2010;3:83–95.
- [12] Aboody KS, Najbauer J, Metz MZ, et al. Neural stem cell-mediated enzyme/prodrug therapy for glioma: preclinical studies. *Science Transl Med.* 2013;5:184ra159.
- [13] Pessina A, Piccirillo M, Mineo E, et al. Role of SR-4987 stromal cells in the modulation of doxorubicin toxicity to in vitro granulocyte-macrophage progenitors (CFU-GM). *Life Sci.* 1999;65:513–523.
- [14] Zhao Y, Tang S, Guo J, et al. Targeted delivery of doxorubicin by nano-loaded mesenchymal stem cells for lung melanoma metastases therapy. *Sci Rep.* 2017;7:44758.
- [15] Pessina A, Bonomi A, Cocce V, et al. Mesenchymal stromal cells primed with paclitaxel provide a new approach for cancer therapy. *PloS One.* 2011;6:e28321.
- [16] Sasportas LS, Kasmieh R, Wakimoto H, et al. Assessment of therapeutic efficacy and fate of engineered human mesenchymal stem cells for cancer therapy. *Proc Natl Acad Sci USA.* 2009;106:4822–4827.
- [17] Li L, Huang X, Liu T, et al. Overcoming multidrug resistance with mesoporous silica nanorods as nanocarrier of doxorubicin. *J Nanosci Nanotech.* 2012;12:4458–4466.
- [18] Chithrani BD, Ghazani AA, Chan WC. Determining the size and shape dependence of gold nanoparticle uptake into mammalian cells. *Nano Lett.* 2006;6:662–668.
- [19] Pittenger MF, Mackay AM, Beck SC, et al. Multilineage potential of adult human mesenchymal stem cells. *Science.* 1999;284:143–147.
- [20] Dominici M, Le Blanc K, Mueller I, et al. Minimal criteria for defining multipotent mesenchymal stromal cells. The international society for cellular therapy position statement. *Cytotherapy.* 2006;8:315–317.
- [21] Xue J, Zhao Z, Zhang L, et al. Neutrophil-mediated anticancer drug delivery for suppression of postoperative malignant glioma recurrence. *Nature Nanotech.* 2017;12:692–700.
- [22] Anari E, Akbarzadeh A, Zarghami N. Chrysin-loaded PLGA-PEG nanoparticles designed for enhanced effect on the breast cancer cell line. *Artif Cells Nanomed Biotechnol.* 2016;44:1410–1416.
- [23] Brannon-Peppas L, Blanchette JO. Nanoparticle and targeted systems for cancer therapy. *Adv Drug Deliv Rev.* 2004;56:1649–1659.
- [24] Peer D, Karp JM, Hong S, et al. Nanocarriers as an emerging platform for cancer therapy. *Nat Nanotechnol.* 2007;2:751–760.
- [25] Jain RK, Stylianopoulos T. Delivering nanomedicine to solid tumors. *Nature reviews. J Clin Oncol.* 2010;7:653–664.
- [26] Herizchi R, Abbasi E, Milani M, et al. Current methods for synthesis of gold nanoparticles. *Artif Cells Nanomed Biotechnol.* 2016;44:596–602.
- [27] Torchilin V. Tumor delivery of macromolecular drugs based on the EPR effect. *Adv Drug Deliv Rev.* 2011;63:131–135.
- [28] Niu M, Naguib YW, Aldayel AM, et al. Biodistribution and in vivo activities of tumor-associated macrophage-targeting nanoparticles incorporated with doxorubicin. *Mol Pharmaceutics.* 2014;11:4425–4436.
- [29] Minchinton AI, Tannock IF. Drug penetration in solid tumours. *Nature reviews. Cancer.* 2006;6:583–592.
- [30] Huang X, Peng X, Wang Y, et al. A reexamination of active and passive tumor targeting by using rod-shaped gold nanocrystals and covalently conjugated peptide ligands. *ACS Nano.* 2010;4:5887–5896.
- [31] Gao Z, Zhang L, Hu J, et al. Mesenchymal stem cells: a potential targeted-delivery vehicle for anti-cancer drug, loaded nanoparticles. *Nanomedicine.* 2013;9:174–184.
- [32] Park JS, Suryaprakash S, Lao YH, et al. Engineering mesenchymal stem cells for regenerative medicine and drug delivery. *Methods.* 2015;84:3–16.
- [33] Ackova DG, Kanjevac T, Rimondini L, et al. Perspectives in engineered mesenchymal stem/stromal cells based anti-cancer drug delivery systems. *Recent Pat Anticancer Drug Discov.* 2016;11:98–111.
- [34] Armulik A. Splice variants of human beta 1 integrins: origin, biosynthesis and functions. *Front Biosci.* 2002;7:d219–d227.
- [35] Ebrahim EK, Assem MM, Amin AI, et al. FLT3 internal tandem duplication mutation, cMPL and CD34 expressions predict low survival in acute myeloid leukemia patients. *Ann Clin Lab Sci.* 2016;46:592–600.
- [36] Hansen KR, Resta R, Webb CF, et al. Isolation and characterization of the promoter of the human 5'-nucleotidase (CD73)-encoding gene. *Gene.* 1995;167:307–312.
- [37] Ince S, Kutsch M, Shydlovskiy S, et al. The human guanylate-binding proteins hGBP-1 and hGBP-5 cycle between monomers and dimers only. *Febs J.* 2017;284:2284–2301.
- [38] Jacobsen M, Schweer D, Ziegler A, et al. A point mutation in PTPRC is associated with the development of multiple sclerosis. *Nat Genet.* 2000;26:495–499.
- [39] Leyton L, Hagood JS. Thy-1 modulates neurological cell-cell and cell-matrix interactions through multiple molecular interactions. *Adv Neurol.* 2014;8:3–20.
- [40] Stalhammar ME, Sindelar R, Douhan HL. Neutrophil receptor response to bacterial N-formyl peptides is similar in term newborn infants and adults in contrast to IL-8. *Scand J Immunol.* 2016;84:332–337.